Farm tractors with suspended front axle: Anti-dive and anti-lift characteristics

Massimiliano Gobbi, Gianpiero Mastinu, Giorgio Previati *

Politecnico di Milano, Department of Mechanical Engineering, Milan, Italy

Received 16 June 2014; received in revised form 2 October 2014; accepted 20 October 2014
Available online 12 November 2014

1. Introduction

In conventional vehicles, the body pitch attitude during braking (dive) or acceleration (lift) depends on many parameters, mainly on the longitudinal acceleration [6]. The inertial force acting at the centre of gravity of the vehicle because of the longitudinal acceleration is equal (and opposite) to the total longitudinal force acting at the contact patches of the tyres. The combined effect of these forces causes a variation of the vertical forces at the tyres and a torque around the pitch axis is applied to the vehicle. In general, due to this torque, an important pitch of the body occurs, which is strongly related to the geometry of the suspension system [5].

For vehicles with two suspended axes, such as cars, the anti-dive problem is extensively discussed in [1–9]. The attitude of the vehicle during braking and acceleration (anti-dive and anti-lift characteristics), is often analysed by means of a in-plane model of the vehicle [1,4,6,9]. The vehicle body is described as a rigid body connected to the front and rear wheels by means of massless links. The wheels are considered rigid and without mass. By this description, the vehicle body has only three degrees of freedom, namely longitudinal, vertical and pitch. The longitudinal motion is constrained by giving the longitudinal acceleration or deceleration. In [1], not only the steady state condition is considered but also the transient behaviour.

From the mentioned models, it turns out that particular geometric configurations of the suspensions exist to fully avoid vehicle pitch while braking (anti-dive configuration) or while accelerating (anti-lift configuration). According to such models, the resultants of the external forces at the tyres should balance the inertial force without creating a pitch torque [7]. In case of brakes located on the wheel

* Corresponding author. Tel.: +39 02 2399 8606; fax: +39 02 2399 8263.
E-mail address: giorgio.previati@polimi.it (G. Previati).

List of symbols

x	longitudinal reference axis (positive toward the front of the vehicle)
z	vertical reference axis (positive upwards)
φ	pitch angle of the vehicle
$\ddot{x}$ and $\ddot{\varphi}$	longitudinal and pitch accelerations
G	centre of gravity of the vehicle and origin of the reference system
O	centre of the rear axle
A	longitudinal (virtual) pole of the front suspension
R_f and R_r	front and rear wheel radii
l	wheelbase
l_f and l_r	distances of the front and rear wheel centres from the centre of gravity in the longitudinal direction
l_{sf}	distance of the longitudinal pole of the front suspension from the centre of the front wheels
h	height of the centre of gravity
h_{sf} and h_{rs}	heights of the longitudinal poles of the front and rear axles ($h_{rs} = R_r$)
k_f and r_f	stiffness and damping of the front suspension
γ	slope of the 100% anti-dive axle
h_0	vertical shift of the 100% anti-dive axle from the ground
B_f and B_r	braking force at the front and rear axles
T_f and T_r	traction force at the front and rear axles
F_{xf} and F_{xf}	variation of the longitudinal forces at the body for the front and rear axles
Z_f	variation in the front vertical force at contact patch
F_{zf}	variation in the front vertical force at the body
F_{zr}	variation in the rear vertical force at contact patch equal to the variation of the rear vertical force at the body
M_f, M_f' and M_f''	traction and braking torques at the front axle (acting on the wheel, on the body and on the hub, respectively)
M_r	traction or braking torque at the rear axle
F_f	force of the spring and damper element of the front suspension
J	tractor body pitch moment of inertia
τ	planetary gear set ratio (ratio between the angular speed of the output and input shafts)
k_{tf} and k_{tr}	radial stiffness of the front and rear tyres, respectively

hubs, the pitch centre should be at the same height of the centre of gravity of the vehicle [1,4,9]. If the brakes are located on the body, the reaction torque on the body has to be taken into account and the pitch centre of the vehicle should be located above the centre of gravity of a quantity equal to the tyre radius [4].

The anti-lift configuration depends on the kind of driveline of the vehicle [4,6]. For a front wheel drive, the pitch centre is located above the rear axle, for a rear wheel drive above the front axle [5]. For a four-wheel drive, the centre of pitch is between the two axles in a position depending on the traction-force distribution [4,6].

As pointed out in [4], to avoid pitch while accelerating, different heights of the centre of pitch are required if dependent or independent suspension schemes (rigid axles) are adopted. (In the first case there is a case similar to the one of brakes located at the wheel hubs, in the latter a case similar to brakes on board of the vehicle body, see [9])

In conventional farm tractors without an actual suspension system, the body attitude during braking or acceleration is given by the deformation of the tyres. If at least one suspension system is introduced (usually at the front axle), the suspension system allows for larger pitch movements. The location of the pitch centre depends on the geometry of the suspension and influences the amount of pitch during braking and acceleration.

Referring to anti-dive and anti-lift characteristics, with respect to cars, farm tractors present two main differences.

Firstly, farm tractors are generally fitted with just one suspension system at the front axle, while the rear axle is rigidly connected to the body. This layout gives a strong coupling between vertical and pitch motions.

The second difference is related to the driveline. In case of four-wheel drive, cars usually have a transfer unit which gives a known traction-force distribution between the front and rear axles [5]. Farm tractors do not have such transfer box but the two axles are rigidly connected [10]. Traction-force distribution and brake balance depend on the current motion of the vehicle, that is the torque at each axle depends on the longitudinal slip rate of the front and rear tyres. Moreover, farm tractors have a planetary gear set located on each wheel hub. This implies that a reaction torque is always present on the hub even in the case in which the brakes are located on the body.

The literature on anti-dive and anti-lift properties of farm tractor suspensions is somewhat limited. In [11] the anti-dive characteristic of the front axle suspension of a farm tractor is considered in order to optimise the active control of the suspension. In such paper, the effect of the driveline on the anti-dive behaviour of the suspension has not been considered but the usual formulas for cars have been used as first guess. The simulations show that a proper setting of the anti-dive characteristic can significantly improve the performance of the suspension in terms of working space, pitch and vertical displacement while reducing the forces acting on the actuator. In [12] a

complete model of the farm tractor, including driveline, is used to evaluate the pitch variation during brake.

In this paper the geometrical features of the suspension system required to avoid the pitching of the farm tractor body are derived. The derived analytical formulae can be useful for the concept design of farm tractors with a front suspension system.

The anti-dive characteristics of the front suspension are studied both for the two-wheel-drive (4×2) and for the four-wheel-drive (4×4) arrangements of the driveline system.

The anti-lift characteristics of the front axle suspension are assessed for the more complex four wheel drive (4×4) arrangement. The behaviour of the farm tractor in case of two-wheel-drive (4×2) is derived as special case.

2. Vehicle model

In Fig. 1 a schematic representation of a farm tractor is reported. The presented analytical model is derived accordingly to the following hypotheses, (as stated in [1] with reference to the analysis of the anti-dive characteristics of a car):

- The model takes into account only the x–z plane of the vehicle (where x and z are the longitudinal and vertical axes respectively).
- The deformation of the tyres is neglected, i.e. rigid tyres are considered.
- The longitudinal acceleration $\ddot{x}$ is given.
- The rear wheel hubs are rigidly connected to the body.
- The suspension is represented by a rigid massless link between the wheel and the body. The link, which represent a virtual arm connecting the wheel centre with the longitudinal pole on the body, is rigidly fixed to the wheel hub and can rotate with respect to the body. By this schematization, the link (or virtual arm) can transmit to the body only forces (along x and z) while it can transmit forces and torques to the hub.
- The front axle elastokinematics is described by equivalent stiffness and damping [1]. The equivalent spring-damper element of the front suspension acts between the centre of the wheel and the body, only in the vertical direction.
- The line of action of the 100% anti-dive line is described by the slope angle γ and the vertical shift h_0 (Fig. 1).
- Contact forces (B_f, B_r, T_f, T_r, Z_f and F_{zr}) are variations with respect to the equilibrium condition. That is, since the model is linear, the steady-state forces are not considered in the model.

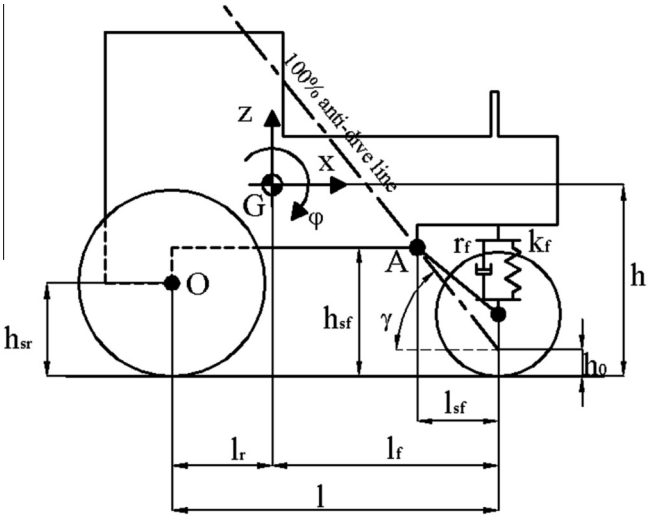

Fig. 1. Scheme of a farm tractor fitted with a front suspension. The depicted case represents a 100% anti-dive configuration, the 100% anti-dive line passes through the longitudinal pole of the suspension A. h_0 vanishes if the front brake reaction torque is applied at the front suspension arms in a rear wheel drive farm tractor.

This model can describe any kind of suspension [1] (see Appendix 1). The effect of the driveline and of the location of the brakes can be taken into account by correctly applying the reaction torques on the links representing the suspension system.

The model considers a farm tractor with a rigid body and no trailer. The presence of implements rigidly connected to the tractor body can be considered by simply changing the tractor body centre of gravity location and pitch moment of inertia to include the effect of the implement. Implements, such as ploughs, that present deformable modes with respect to the traction body or trailers are not included in the model.

According to the first four hypotheses, the model has only one degree of freedom. In fact, a rigid body moving in the vertical plane has three degrees of freedom, namely x, z and φ. Since x is given and z and φ are related, only one degree of freedom is permitted.

The rigid tyre hypothesis has been introduced in order to consider only the body pitch due to the suspension kinematic. As tractors usually have massive tyres with relative large deflections, a certain amount of pitch is present even if without any suspension deformation. The effect of tyre deformations will be considered in the last section of the paper.

By considering rigid tyres and rear wheel hubs rigidly connected to the body, the centre of rotation of the tractor is point O of Fig. 1. Referring to the symbols of Fig. 1, for small displacements, the linearized relationship between the vertical displacement z and the rotation angle φ is

$$z = -l_r \varphi \tag{1}$$

It must be observed that, as Eq. (1) relates vertical and pitch degrees of freedom, the model considered for the description of the pitch behaviour of a farm tractor during braking and acceleration is quite different from the corresponding model for conventional vehicles (which has two independent degrees of freedom, namely heave and pitch). Moreover, given the complexity of the driveline, the brake reaction torques have to be split between wheel hubs and

tractor body and, when a 4×4 driveline is considered, reaction torques are coupled between front and rear axle. This coupling carries out particular behaviours typical of farm tractors that cannot be observed in conventional vehicles and are not described by the commonly used models presented in [1,4–9].

3. Anti-dive

This section is devoted to the analysis of the anti-dive properties of a farm tractor with a front axle suspension. In the following, both the 4×2 (two wheel drive, actually rear wheel drive) and the 4×4 drivelines are taken into account, separately.

3.1. Farm tractor with rear wheel drive (4×2)

Fig. 2 shows the forces acting on the body, suspension and wheels of the vehicle while braking. Referring to the symbols in the figure and remembering the relationship between z and φ reported in Eq. (1), the dynamic equilibrium of the body of the tractor can be written as

$$\begin{cases} m\ddot{x} = F_{xf} + F_{xr} \\ m\ddot{x}(h - h_{sr}) + J\ddot{\varphi} = -F_f l - F_{zf}(l - l_{sf}) + F_{xf}(h_{sf} - h_{sr}) \\ \qquad + M_r \end{cases} \tag{2}$$

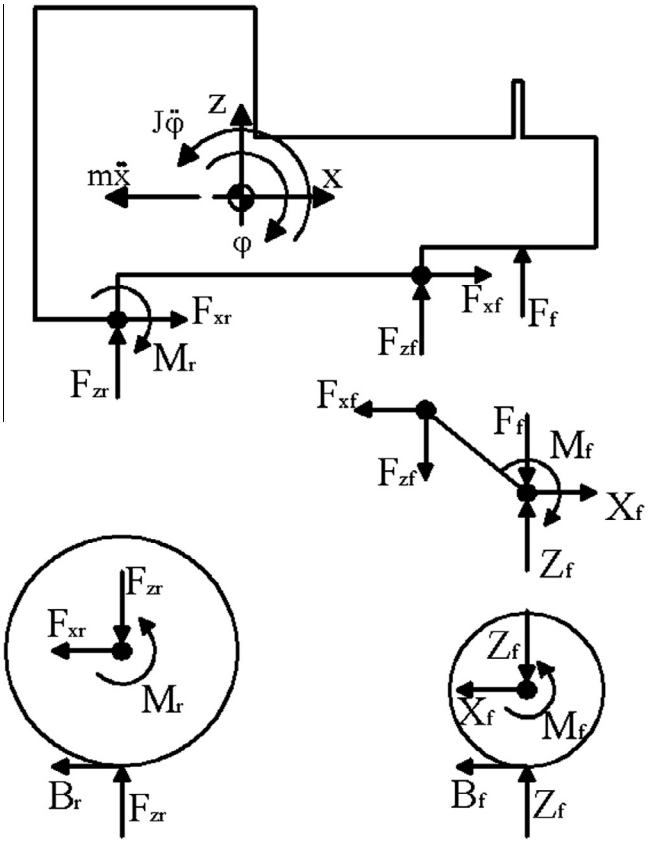

Fig. 2. Forces and torques acting on a 4×2 farm tractor, front brakes at the hub.

where the first equation describes the equilibrium in the x direction and the second equation the rotation around point O. m and J are the mass and the moment of inertia of the body of the tractor, respectively.

By considering the front wheels, the following equilibria can be derived

$$\begin{cases} B_f + X_f = 0 \\ M_f - B_f R_f = 0 \end{cases} \tag{3}$$

where R_f is the radius of the front wheels. For the rear wheels

$$\begin{cases} B_r + F_{xr} = 0 \\ M_r - B_r R_r = 0 \end{cases} \tag{4}$$

with R_r the radius of the rear wheels (since the rear wheel is rigidly connected to the body, according to the symbols of Fig. 1, $R_r = h_{sr}$). From the equilibrium of the arm of the front suspension we obtain

$$\begin{cases} X_f - F_{xf} = 0 \\ M_f - F_{zf} l_{sf} - F_{xf}(h_{sf} - R_f) = 0 \end{cases} \tag{5}$$

The vertical force acting on the suspension can be computed as

$$F_f = k_f l\varphi + r_f l\dot{\varphi} \tag{6}$$

where k_f and r_f are the stiffness and damping coefficient of the front suspension respectively. $l\varphi$ and $l\dot{\varphi}$ are the linearized vertical displacement and velocity of the point of connection between the spring-damper element and the body, respectively. Notice that, since the wheel is rigid, this displacement and velocity are equal to the deformation and velocity of deformation of the spring-damper element. By substituting Eqs. (3)–(6) in Eq. (2), the dynamic equilibrium of the body of the tractor can be rewritten as

$$\begin{cases} m\ddot{x} = -B_f - B_r \\ m\ddot{x}(h - h_{sr}) + J\ddot{\varphi} = -(k_f l\varphi + r_f l\dot{\varphi}) l - B_f \frac{h_{sf}}{l_{sf}}(l - l_{sf}) \\ \qquad -B_f(h_{sf} - h_{sr}) + B_r h_{sr} \end{cases} \tag{7}$$

replacing the first of Eq. (7) in the second and rearranging

$$J\ddot{\varphi} + r_f l^2 \dot{\varphi} + k_f l^2 \varphi = -m\ddot{x} \cdot \left(h - h_{sr} - \frac{B_f}{B_f + B_r} \frac{h_{sf}}{l_{sf}} l + \frac{B_f}{B_f + B_r} h_{sr} + \frac{B_r}{B_f + B_r} h_{sr} \right) \tag{8}$$

observing that $\frac{B_f}{B_f + B_r} h_{sr} + \frac{B_r}{B_f + B_r} h_{sr} = h_{sr}$, Eq. (8) can be simplified as

$$J\ddot{\varphi} + r_f l^2 \dot{\varphi} + k_f l^2 \varphi = -m\ddot{x} \cdot \left(h - \frac{B_f}{B_f + B_r} \frac{h_{sf}}{l_{sf}} l \right) \tag{9}$$

The condition for having a null rotation angle of the body during braking is that the right side of Eq. (9) has to vanish [1], thus

$$\frac{h_{sf}}{l_{sf}} = \frac{h}{l} \frac{B_f + B_r}{B_f} \tag{10}$$

Referring to Fig. 1, the slope angle γ and the vertical shift h_0 of the 100% anti-dive line are

$$\gamma = \arctan\left(\frac{h_{sf}}{l_{sf}}\right) = \arctan\left(\frac{h}{l}\frac{B_f + B_r}{B_f}\right), \quad h_0 = 0 \tag{11}$$

Eq. (11) gives the slope angle of the line where the longitudinal pole of the front suspension required to have 100% of anti-dive has to lie, i.e. if this condition is satisfied, the tractor will have no pitch angle during braking. This is the same condition that is given for the front suspension arm of a car with brakes on the hubs [1,9].

Eq. (11) is quite general and does not depend on the actual architecture of the brake system. For any given braking system, the brake balance between front and rear axles is known, thus the ratio $(B_f + B_r)/B_r$ can be computed and the 100% anti-dive condition can be derived. The designer can then choose the desired anti-dive percentage. It can be observed that in case the ratio $(B_f + B_r)/B_r$ is not constant (for instance if a pressure limiter is present on the rear axle), different 100% anti-dive conditions can be computed.

In Fig. 3, the forces and torques acting on the farm tractor when the front brakes are located on the body are reported. Notice that the braking torque M_f' applied by the brakes is multiplied by the gear ratio of the planetary gears on the hubs. Thus a reaction torque M_f'' arises on the hubs. The braking torque on the wheel is

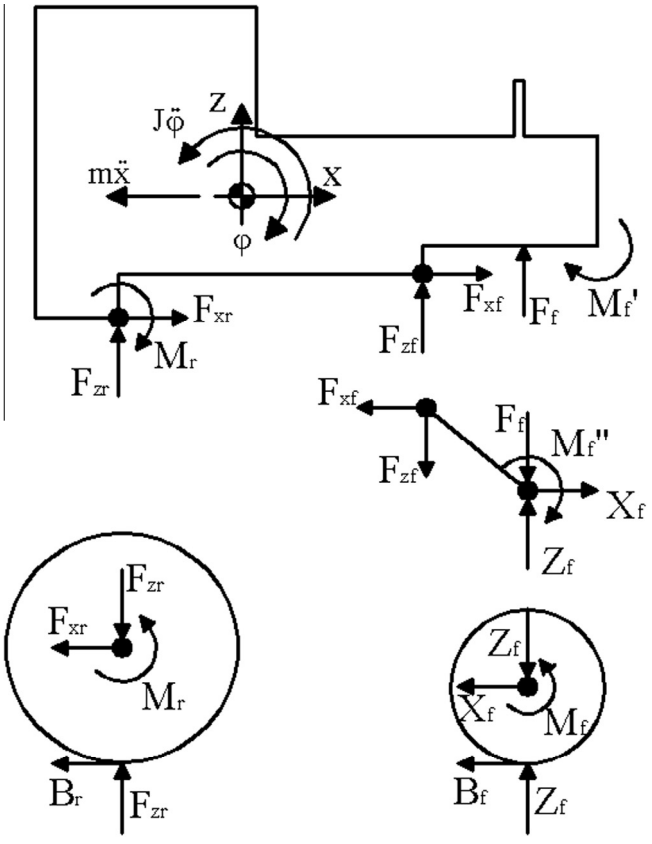

Fig. 3. Forces and torques acting on a farm 4 × 2 farm tractor brakes on the body.

$$M_f = \frac{M_f'}{\tau} \tag{12}$$

where τ is the ratio of the planetary gear set ($\tau < 1$). The reaction torque on the hubs is

$$M_f'' = \frac{1-\tau}{\tau} M_f' \tag{13}$$

Considering M_f', Eq. (2) can be rewritten as

$$\begin{cases} m\ddot{x} = F_{xf} + F_{xr} \\ m\ddot{x}(h - h_{sr}) + J\ddot{\varphi} = -F_f l - F_{zf}(l - l_{sf}) + F_{xf}(h_{sf} - h_{sr}) \\ \qquad\qquad + M_r + M_f' \end{cases} \tag{14}$$

and Eq. (5)

$$\begin{cases} X_f - F_{xf} = 0 \\ M_f'' - F_{zf} l_{sf} - F_{xf}(h_{sf} - R_f) = 0 \end{cases} \tag{15}$$

By replacing Eqs. 3, 4, 6 and 15 into Eq. (14) and rearranging we obtain

$$\begin{cases} m\ddot{x} = -B_f - B_r \\ m\ddot{x}(h - h_{sr}) + J\ddot{\varphi} = -(k_f l\varphi + r_f l\dot{\varphi})l - B_f\frac{(h_{sf} - \tau R_f)}{l_{sf}}(l - l_{sf}) \\ \quad -B_f(h_{sf} - h_{sr}) + B_r h_{sr} + \tau B_f R_f \end{cases} \tag{16}$$

replacing the first of Eq. (16) in the second, rearranging and simplifying

$$J\ddot{\varphi} + r_f l^2\dot{\varphi} + k_f l^2\varphi = -m\ddot{x}\cdot\left(h - \frac{B_f}{B_f + B_r}\frac{h_{sf}}{l_{sf}}l + \frac{B_f}{B_f + B_r}\frac{\tau R_f}{l_{sf}}l\right) \tag{17}$$

Finally, the condition for 100% anti-dive is

$$\frac{h_{sf}}{l_{sf}} = \frac{h}{l}\frac{B_f + B_r}{B_f} + \frac{R_f}{l_{sf}}\tau \tag{18}$$

Referring to Fig. 1, the slope angle γ and the vertical shift h_0 of the 100% anti-dive line are

$$\gamma = \arctan\left(\frac{h_{sf}}{l_{sf}}\right) = \arctan\left(\frac{h}{l}\frac{B_f + B_r}{B_f}\right), \quad h_0 = \tau R_f \tag{19}$$

For $\tau = 1$ Eq. (18) gives the same conditions for 100% anti-dive of a car with brakes located on the body [4,9]. The presence of a planetary gear on the hub reduces the vertical shift of the 100% anti-dive line with respect to a car without any reduction in the hubs. The higher the reduction gear ratio of the planetary gear (the lower τ), the lower the vertical shift h_0.

3.2. Farm tractor with four wheel drive (4 × 4)

In farm tractors, 4 × 4 is obtained by rigidly connecting the front and rear driveshafts, i.e. no central differential is present [10]. According to [10] for optimal traction performances, the gear ratio between the front and rear axles should be chosen to have the same theoretical speed of

front and rear wheels. However, due to tyre mismatch, wear or other causes, this situation is seldom achieved and differences up to 10% can be found between the two speeds [10]. Therefore, while running on an even straight road, the wheels with the higher speed pull the farm tractor, while the other wheels exert a force in the opposite direction [11]. The braking torques are split between the two shafts depending on the actual vertical forces and longitudinal slips acting at the tyres. The very complex behaviour of such a driveline during braking will be discussed in the following.

In most farm tractors, when high braking torques are applied, the brake system is designed in order to transfer braking torque from the rear axle to the front axle. In some cases, the front brakes are removed and the brake torque is applied only to the rear axle and then transferred by the driveline to the front axle.

Referring to the symbols of Fig. 3, the following definitions apply to the 4 × 4 case.

M_f' = braking torque coming from the drive line. It can be generated by the rear brakes or/and by front brakes located on the body (if present).
M_f'' = braking torque generated by front brakes located at the front hubs (if present) plus the reaction torque on the front axle due to the transmission of M_f' and of the braking torque generated at the front hubs through the planetary gear.
M_f = total braking torque on the front wheels.

Defining M_{brk} as the braking torque of the front brakes located at the front axle, M_f can be computed as

$$M_f = \frac{M_f'}{\tau} + \frac{M_{\text{brk}}}{\tau} \tag{20}$$

where τ is the gear ratio of the planetary gear. Since the brakes are located before the hub reduction, M_{brk} is divided by τ. The following ratio can be defined

$$\alpha = \frac{M_f'}{M_{\text{brk}}} \tag{21}$$

where α represents the ratio between the braking force generated on the body (by the rear brakes and/or by brakes located on the body) and the braking force generated on the front axle (by front brakes located on the front hubs). From Eqs. (20) and (21), M_f' can be expressed as

$$M_f' = \frac{\tau\alpha}{1+\alpha} M_f \tag{22}$$

and by considering the definition of M_f' and M_f'', it can be stated that

$$M_f' + M_f'' = M_f \quad \Rightarrow \quad M_f'' = M_f - M_f' = \frac{1+\alpha-\tau\alpha}{1+\alpha} M_f \tag{23}$$

The equilibrium equations of the body of the farm tractor and of the front axle are formally identical to Eqs. (14) and (15) respectively. By replacing Eqs. 3, 4, 6 and 15 into Eq. (14) and by considering Eqs. (22) and (23), we obtain

$$\begin{cases} m\ddot{x} = -B_f - B_r \\ m\ddot{x}(h - h_{sr}) + J\ddot{\varphi} = -\left(k_f l\varphi + r_f l\dot{\varphi}\right)l \\ \qquad -B_f\left(h_{sf} - \frac{\tau\alpha}{1+\alpha}R_f\right)\frac{(l-l_{sf})}{l_{sf}} - B_f\left(h_{sf} - h_{sr}\right) \\ \qquad +B_r h_{sr} + \frac{\tau\alpha}{1+\alpha}B_f R_f \end{cases} \tag{24}$$

replacing the first of Eq. (24) in the second, rearranging and simplifying

$$J\ddot{\varphi} + r_f l^2\dot{\varphi} + k_f l^2\varphi = -m\ddot{x}\cdot\left(h - \frac{B_f}{B_f+B_r}\frac{h_{sf}}{l_{sf}}l + \frac{B_f}{B_f+B_r}\frac{\tau\alpha}{1+\alpha}\frac{R_f}{l_{sf}}l\right) \tag{25}$$

Finally, the condition for 100% anti-dive is

$$\frac{h_{sf}}{l_{sf}} = \frac{h}{l}\frac{B_f+B_r}{B_f} + \frac{\tau\alpha}{1+\alpha}\frac{R_f}{l_{sf}} \tag{26}$$

Referring to Fig. 1, the slope angle γ and the vertical shift h_0 of the 100% anti-dive line are

$$\gamma = \arctan\left(\frac{h_{sf}}{l_{sf}}\right) = \arctan\left(\frac{h}{l}\frac{B_f+B_r}{B_f}\right), \quad h_0 = \frac{\tau\alpha}{1+\alpha}R_f \tag{27}$$

Eq. (27) takes into account the effects of the drive line and of the planetary gear on the front axle. If $\alpha = 0$, Eq. (27) assumes the same expression of Eq. (11), representing the case of a 4 × 2 where no braking torque is transmitted through the drive line. If $\alpha \to \infty$ Eq. (27) assumes the same expression of Eq. (19), representing the limit case in which no brake is present on the front axle and all the braking force is originated by brakes on the body (or transmitted to the front axle by the driveline).

For $\alpha > 0$, both the brakes on the front wheels hubs and the driveline contribute to the braking torque, the vehicle shows a dynamic behaviour in between with respect to these two limit cases.

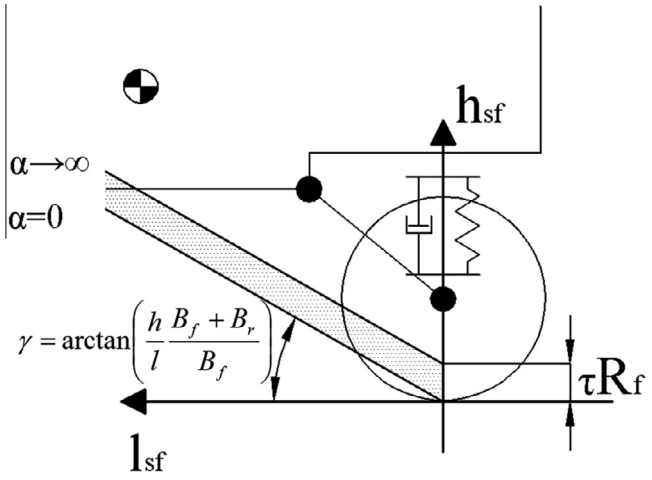

Fig. 4. Geometrical representation of the 100% anti-dive condition for a 4 × 4 tractor and $\alpha \geqslant 0$.

In Fig. 4 a graphical representation of anti-dive conditions for a tractor with 4×4 and $\alpha \geqslant 0$ is depicted. The relationship h_{sf} as function of l_{sf} is shown.

$$h_{sf} = \frac{h}{l}\frac{B_f + B_r}{B_f} l_{sf} + \frac{\tau\alpha}{1+\alpha} R_f \tag{28}$$

This relationship is a straight line with slope depending on the longitudinal forces. The vertical shift h_0 depends on the type of driveline and brakes. In particular, for $\alpha \geqslant 0$ the following cases may arise (see Fig. 4):

- If $\alpha = 0$ then $h_0 = 0$. This is the case corresponding to brakes located on the wheel hub and no torque is transmitted through the driveline.
- If $\alpha > 0$ then $0 < h_0 \leqslant \tau R_f$ (dotted region of Fig. 4). The limit case $h_0 = \tau R_f$ is obtained for $\alpha \to +\infty$. In this limit case, no braking torque is originated at the wheel hub.

The value of h_0 is usually between zero and one fourth or one sixth of the radius of the tyre. In fact, the gear ratio on the front axle (τ) is usually between 1/4 and 1/6.

The angle γ is function of the relative value of the longitudinal forces applied to the front and to the rear axle. Since the torques in the driveline are not statically determined, these values depend on the braking torque, the actual friction coefficient, the vertical load and the deformation of the tyres (in other words, on tyre characteristics). In such a case, γ can change even during a single braking manoeuvre.

The condition $\alpha \geqslant 0$ is not the only one possible. In fact, if the front brakes apply a torque exceeding the braking force that the front wheels can generate, part of this torque is transmitted to the rear axle and M_f' is negative. Since M_{brk} is positive, according to Eq. (21), α assumes negative values.

Depending on the relative values of M_f' and M_{brk}, from a mathematical point of view three scenarios can be identified for the angle γ when $\alpha < 0$

- $-1 < \alpha < 0$ (that is $-M_{\mathrm{brk}} < M_f' < 0$): $B_f > 0$, γ is smaller than 90°.
- $\alpha = -1$ (that is $M_f' = -M_{\mathrm{brk}}$): B_f is equal to zero and γ is equal to 90°.
- $\alpha < -1$ (that is $M_f' < -M_{\mathrm{brk}}$): B_f is negative but $B_r + B_f$ is positive (the vehicle is braking). γ is between −90° and 0°.

Among these three conditions, only the first one could have a practical interest. The second one is a limit case in which the front axle has a null friction coefficient and all the braking torque is transmitted to the rear axle. The third case has no physical meaning.

According to Eq. (27), for $\alpha < 0$ the vertical shift h_0 is always negative. That is, the intersection point between the 100% anti-dive axis and the vertical axis passing through the centre of the front wheel is below road level. For $-1 < \alpha < 0$, h_0 is between 0 (road level, for $\alpha = 0$) and $-\infty$ (for $\alpha \to -1$).

4. Numerical validation

The analytical formulae for the prediction of the anti-dive configuration of the vehicle have been validated by means of a multi-body model of a complete farm tractor (see Appendix 2 for model description and validation). The model employed for the validation is based on the model of a standard farm tractor without front suspension presented in [11,14,15]. This model considers all the subsystems of the vehicle including a complete model of the driveline system (both 4×2 and 4×4 drive). The tyre characteristics are the ones measured in [14] on dry asphalt road. The model has been experimentally validated as shown in [15]. A suspension system at the front axle has been included in the model as shown in [12]. For validation purposes, the model has been then simplified by neglecting the aerodynamic forces and considering stiff tyres without rolling resistance (i.e. no drag force opposes to the motion of the vehicle). Model data are reported in Table 1.

Two different braking manoeuvres have been considered, one with acceleration of −0.5 g and one with acceleration of −0.3 g. In both cases, the starting velocity is 15 m/s. The ratio between the front and rear brake torque is equal to 0.5. Braking torques, velocities and accelerations during the two manoeuvres are shown in Fig. 5.

4.1. Two wheel drive (4×2)

Four different configurations of the tractor are considered, two with the brakes located on the wheels hubs and two with the brakes located on the body. For each location of the brakes, the front axle suspension has two configurations: 100% anti-dive configuration and a configuration with longitudinal pole located at the same height of the front wheels centre (horizontal virtual arm).

Fig. 6 shows the total front and rear longitudinal forces in the two considered braking manoeuvres. Since in the 4×2 case the front wheels are not connected to the rear wheels, the longitudinal forces are proportional to the

Table 1
Main parameter values of the multi-body model of the farm tractor.

Parameter	Value
Vehicle mass	2500 kg
Pitch moment of inertia	2000 kg m^2
Wheel base	2.08 m
Centre of gravity height	0.84 m
Front tyre radius	0.45 m
Rear tyre radius	0.66 m
Front suspension stiffness	50,000 N/m
Front suspension damping	10,000 Ns/m
Front axle hub gear ratio	13/63
Rear axle hub gear ratio	12/81
Front axle to rear axle gear ratio	1.0624
Front wheels speed to rear wheels speed ratio	1.009
Distance of the longitudinal pole of the front suspension from the centre of the front wheels (l_{sf})	0.5 m

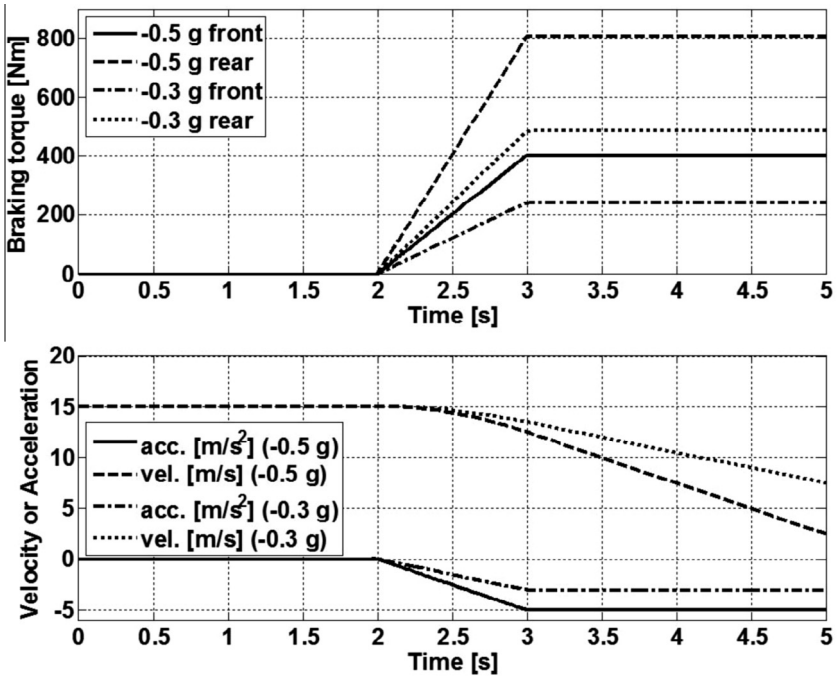

Fig. 5. Braking manoeuvres. Top: applied braking torques. Bottom: velocities and accelerations.

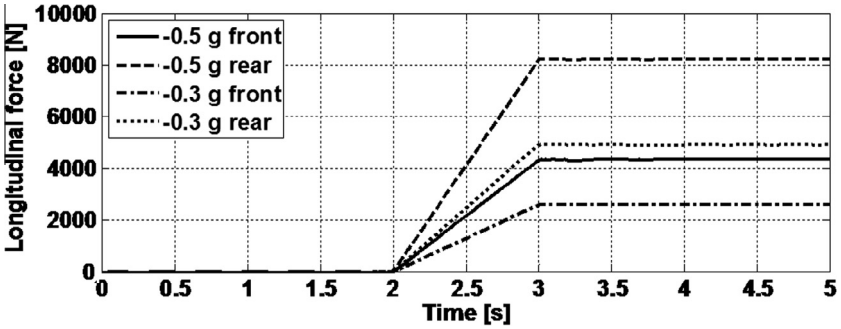

Fig. 6. 4 × 2, longitudinal forces.

applied braking torque on the respective axis and are equal for all the considered configurations. In particular, given the ratio between the front and rear braking torque, the ratio $(B_f + B_r)/B_f$ is constant.

Fig. 7 depicts the pitch angles, for the two manoeuvres, for the two configurations with brakes located on the wheels hubs (top) and on the body (bottom). As expected, the configurations with horizontal virtual arm show a positive pitch angle proportional to the attained level of acceleration. The pitch angles of the configuration with brakes on the body shows a higher pitch angle with respect to the corresponding case with brakes located on the wheels hubs. The configurations with 100% anti-dive have no pitch angle both at steady state and in the transient, independently on the acceleration attained.

In Table 2 the results of the comparison between the analytical and the multi-body models are reported.

4.2. Four wheel drive (4 × 4)

Referring to 4 × 4 farm tractor, only the case of brakes located on the wheel hub is considered (the condition of brakes located on the body can be seen as a particular case).

Fig. 8 shows the total front and rear longitudinal forces in the two considered braking manoeuvres. Since no differential unit is present between the front and rear axle, the longitudinal forces show a complex behaviour. In particular, it can be observed:

- In the first phase of the manoeuvre, when the vehicle is running at constant speed, even without any resistance force acting, the front and rear longitudinal forces are different from zero. In particular, since the speed of the front wheels is higher than that of the rear ones, the total front longitudinal force is a traction force while the rear force is directed against the motion.

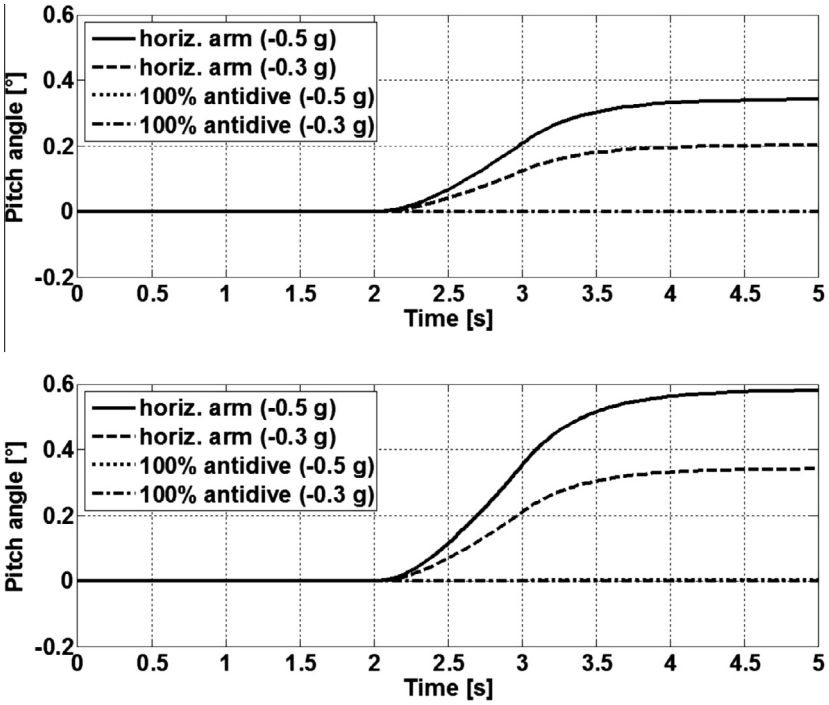

Fig. 7. 4 × 2, pitch angles with and without anti-dive slope of the front suspension. Top: brakes on the wheels hubs. Bottom: brakes on the body.

Table 2
4 × 2: Comparison between the analytical and the multi-body models. The values of h_{sf} for 100% anti-dive configuration are computed by Eqs. (10) and (18), $l_{sf} = 0.5$ m.

Configuration	Accel. [g]	100% anti-dive h_{sf} [mm]	Current h_{sf} [mm]	Anti-dive		φ [°]	
				Analytical (%)	Multi-body (%)	Analytical	Multi-body
Brakes on the hubs, horiz. arms	−0.3	584.7	450	<100	<100	0.20	0.20
	−0.5	584.7	450	<100	<100	0.33	0.35
Brakes on the hubs, 100% anti-dive	−0.3	584.7	584.7	100	100	0.00	0.00
	−0.5	584.7	584.7	100	100	0.00	0.00
Brakes on the body, horiz. arms	−0.3	677.6	450	<100	<100	0.33	0.34
	−0.5	677.6	450	<100	<100	0.55	0.59
Brakes on the body, 100% anti-dive	−0.3	677.6	677.6	100	100	0.00	0.00
	−0.5	677.6	677.6	100	100	0.00	0.00

- In spite of the rear brakes giving a greater braking torque than the front ones, the front total longitudinal braking force at steady state is greater than the rear. The driveline is actually transferring part of the rear braking torque to the front axle.
- At different acceleration levels, the ratio between front and rear forces is not constant. In fact, it depends on the actual state of the vehicle. Accordingly, the ratio $(B_f + B_r)/B_f$ depends on the acceleration level.

Because of such a complex behaviour, a unique 100% anti-dive configuration cannot be defined but it depends, among other parameters, on the acceleration level. In the following, two suspension configurations will be considered for the validation: a configuration set to have 100% anti-dive for the manoeuvre with −0.5 g of acceleration and a suspension with horizontal virtual arm.

Fig. 9 shows the pitch angles for the two configurations of the front axle suspension in the two considered manoeuvres. The configuration with 100% anti-dive at −0.5 g of acceleration shows a null pitch angle at steady state. During the transient, the pitch angle is different from zero. This was expected since the ratio between front and rear longitudinal forces is constantly varying during the transient, requiring different conditions to have 100% anti-dive at each instant. The 100% anti-dive condition applies only at –0.5 g. In fact, with the same configuration, at −0.3 g a positive pitch angle is present. As shown in Table 3, the h_{sf} value of 350 mm (computed by Eq. (28)) gives 100% anti-dive only at −0.5 g. At −0.3 g the computed value of h_{sf} for 100% anti-dive is 387.7 mm. The suspension with horizontal virtual arm shows a negative pitch angle in both cases. In fact, the wheel centre is at 450 mm from the ground, higher than the h_{sf} values for 100% anti-dive computed for both manoeuvres.

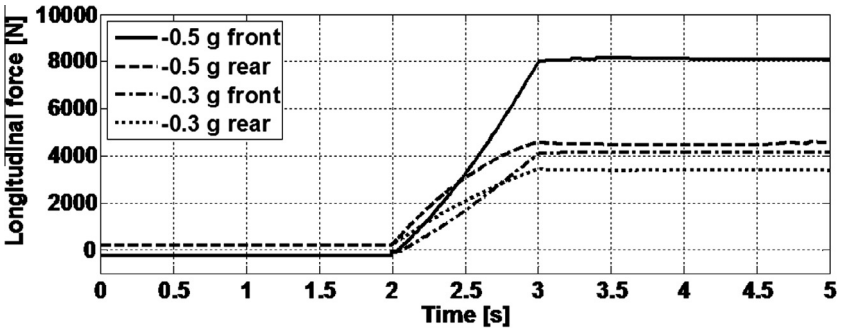

Fig. 8. 4 × 4 driveline, longitudinal forces.

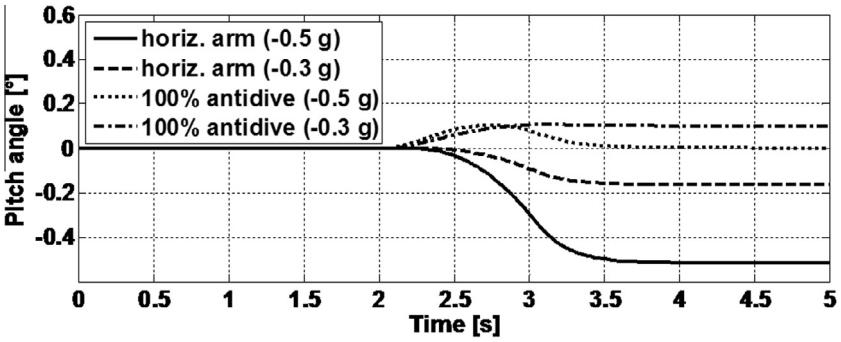

Fig. 9. 4 × 4, pitch angle.

Table 3
4 × 4: Comparison between the analytical and the multi-body models. The values of h_{sf} for 100% anti-dive configuration are computed by Eq. (27), $l_{sf} = 0.5$ m.

Configuration	Accel. [g]	100% anti-dive h_{sf} [mm]	Current h_{sf} [mm]	Anti-dive		φ [°]	
				Analytical (%)	Multi-body (%)	Analytical	Multi-body
Brakes on the hubs, horiz. arms	−0.3	387.7	450	>100	>100	−0.15	−0.16
	−0.5	350.0	450	>100	>100	−0.46	−0.51
Brakes on the hubs, 100% anti-dive	−0.3	387.7	350.0	<100	<100	0.09	0.11
	−0.5	350.0	350.0	100	100	0.00	0.00

Fig. 10 shows the anti-dive parameters of Eq. (28) during the two braking manoeuvres for the configuration with 100% anti-dive at −0.5 g. The plots starts when the braking action starts (at 2 s) because before this instant B_f (longitudinal net braking force at the front axle) and M_{brk} are null. Therefore, γ and α are not defined before this instant.

The slope angle γ (Fig. 1) is reported in Fig. 10A. Two important considerations can be derived. In the first part of the manoeuvre, as the braking action builds up, the ratio $(B_f + B_r)/B_f$ is varying and thus γ varies. This means that in the first part of the braking, the orientation of the line representing the anti-dive condition changes. The second consideration refers to the steady state value. Depending on the entity of the braking action, different steady state values for γ are found.

In Fig. 10B the coefficient α is shown for the two braking manoeuvres. By its definition, coefficient α (Eq. (21)) represents the ratio between the braking torque acting at the front wheels transferred to the front axle by the driveline and the one generated on the hub. If $\alpha < 0$ it means that some of the braking force generated on the front axle is applied to the rear axle, if $\alpha > 0$ it means that some of the braking force generated on the rear axle is applied to the front axle. By inspecting Fig. 10B, it can be observed that during the whole manoeuvres, the driveline provides a certain amount of braking force to the front axle. As the deceleration grows, the vertical load on the front axle grows while the one on the rear axle decreases. The front axle is then capable of more longitudinal force of the rear axle and more braking torque is transferred forwards.

In Fig. 10C the vertical shift h_0 (Fig. 1) of the 100% anti-dive line is depicted. Accordingly to the variation of α in the first part of the manoeuvres h_0 is also changing. At steady state, different values are reached for the two levels of accelerations.

In Fig. 10D the computed height of the longitudinal pole of the suspension h_{sf} (Fig. 1) for 100% anti-dive is reported. According to the variation of γ and h_0 in the first

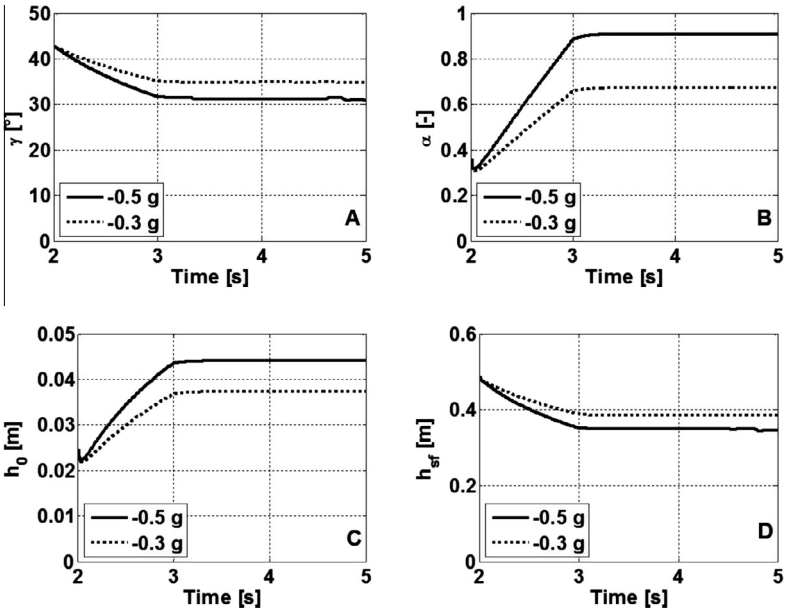

Fig. 10. 4 × 4. Anti-dive parameters during the two braking manoeuvres at two deceleration levels (−0.3 g and −0.5 g). (A) γ angle (see Fig. 1). (B) α parameter (see Eq. (21)). (C) Vertical shift h_0 (see Fig. 1). (D) Height of the longitudinal pole h_{sf} (see Fig. 1) computed for 100% anti-dive ($l_{sf} = 0.5$ m).

part of the manoeuvres h_s is also changing. At steady state, different values are reached for the two levels of accelerations. The steady state value of h_{sf} for the manoeuvre at −0.3 g is higher than the one for the manoeuvre at −0.5 g.

Table 3 shows the comparison between the analytical and the multi-body models.

In such a complex scenario, setting up the anti-dive characteristic of the farm tractor is very difficult. However, the comprehension of the phenomenon is important to choose a good compromise when designing the suspension.

5. Anti-lift

The same approach employed in Section 2 for the computation of the anti-dive characteristic is used in this section to derive the anti-lift characteristic during traction. The forces and torques acting on the farm tractor are reported in Fig. 11. The plots refer to a 4 × 4 tractor with planetary gear on the front axle. Considering independent front wheel suspensions, the dynamic equilibrium of the body can be computed as

$$\begin{cases} m\ddot{x} = F_{xf} + F_{xr} \\ m\ddot{x}(h - h_{sr}) + J\ddot{\varphi} = -F_f l - F_{zf}(l - l_{sf}) + F_{xf}(h_{sf} - h_{sr}) \\ \qquad + M_r + M'_f \end{cases} \tag{29}$$

The relationship defining the equilibrium of the front wheels reads

$$\begin{cases} T_f - X_f = 0 \\ M_f - T_f R_f = 0 \end{cases} \tag{30}$$

where R_f is the radius of the front wheels. For the rear wheels

$$\begin{cases} T_r - F_{xr} = 0 \\ M_r - T_r R_r = 0 \end{cases} \tag{31}$$

with R_r the radius of the rear wheels. From the equilibrium of the arm of the front suspension we obtain

$$\begin{cases} X_f - F_{xf} = 0 \\ M'_f + F_{zf} l_{sf} + F_{xf}(h_{sf} - R_f) = 0 \end{cases} \tag{32}$$

where

$$M_f = \frac{M_f{}'}{\tau} \quad \text{and} \quad M''_f = \frac{1-\tau}{\tau} M'_f \tag{33}$$

where τ is the ratio of the planetary gear ($\tau < 1$). By replacing Eqs. (30)–(33) in Eq. (29), the dynamic equilibrium of the body of the tractor can be rewritten as

$$\begin{cases} m\ddot{x} = T_f + T_r \\ m\ddot{x}(h - h_{sr}) + J\ddot{\varphi} = -(k_f l\varphi + r_f l\dot{\varphi}) l \\ \qquad -T_f \frac{(h_{sf} - \tau R_f)}{l_{sf}}(l - l_{sf}) - T_f(h_{sf} - h_{sr}) + T_r h_{sr} + \tau T_f R_f \end{cases} \tag{34}$$

by replacing the first of Eq. (34) in the second, rearranging and simplifying

$$J\ddot{\varphi} + r_f l^2 \dot{\varphi} + k_f l^2 \varphi = -m\ddot{x} \cdot \left(h - \frac{T_f}{T_f + T_r} \frac{h_{sf}}{l_{sf}} l + \frac{T_f}{T_f + T_r} \frac{\tau R_f}{l_{sf}} l \right) \tag{35}$$

Finally, the condition for 100% anti-lift is

$$\frac{h_{sf}}{l_{sf}} = \frac{h}{l} \frac{T_f + T_r}{T_f} + \frac{R_f}{l_{sf}} \tau \tag{36}$$

For $\tau = 1$, Eq. (36) gives the same condition of a car with 4 × 4 and independent suspensions [4]. The effect of

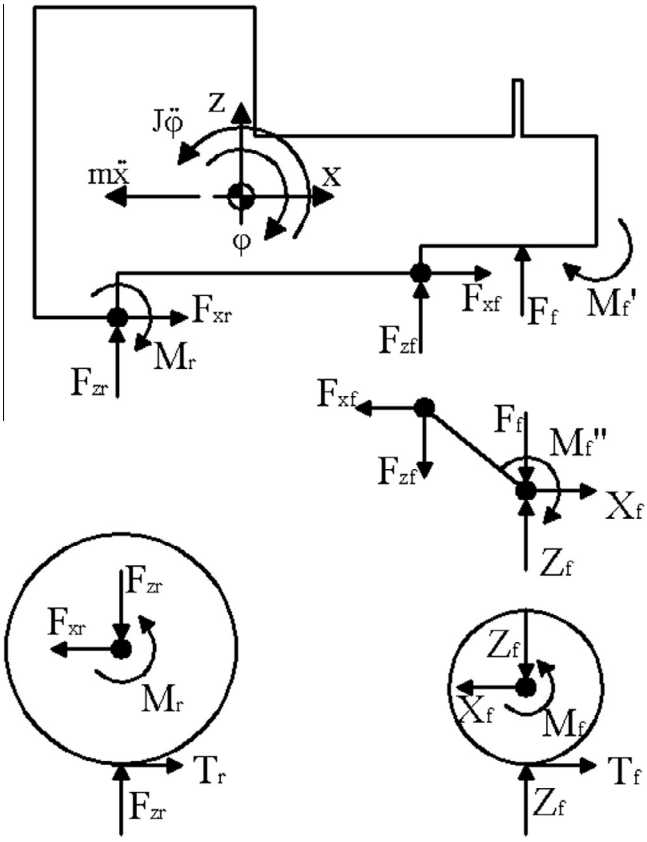

Fig. 11. Forces and torques acting on a 4 × 4 farm tractor.

the presence of a planetary gear on the hub is to reduce the value of h_0. Angle γ is function of the actual values of the front and rear longitudinal forces. By considering the non statically determined drive line, similar considerations with respect to the braking with 4 × 4 can be derived.

In case of a rear wheel drive, the front longitudinal force is vanishing, thus

$$\frac{h_{sf}}{l_{sf}} = \rightarrow \infty \quad \text{as} \quad T_f \rightarrow 0 \tag{37}$$

In this case, the front arm should be vertical. In case of front wheel drive, the longitudinal force on the rear axle is vanishing and the condition for 100% anti-lift is

$$\frac{h_{sf}}{l_{sf}} = \frac{h}{l} + \frac{R_f}{l_{sf}}\tau \tag{38}$$

where if $\tau = 1$, this condition has the same expression of the anti-lift condition for a car [4].

In case of dependent front wheels (i.e. suspended rigid axle) the reaction torque M_f' is vanishing and h_0 is equal to 0.

6. Tyre deformations

In Section 1, one of the hypothesis at the base of the analytical model presented is the assumption of rigid tyres. Current farm tractors are usually equipped with large and massive tyres whose deformations cause non-negligible pitch motions to the vehicle body. The analysis of the dynamic effects of tyre deformations on the pitch motion of the vehicle is behind the scope of this paper. Considering the equilibrium condition, under hypothesis of small displacements, the pitch rotation due to tyres deflections can be added to the pitch rotation due to the suspension deformation.

The body rotation due to tyres deflections can be computed as

$$\varphi_{\text{tyres}} = \frac{m\,\dddot{x}\,h}{2k_{tf}l_f^2 + 2k_{tr}l_r^2} \tag{39}$$

where k_{tf} and k_{tr} are the respective tyre radial stiffnesses for the front and rear tyres. For reasonable values of vehicle parameters, this rotation can be of the order of some tenths of degree. Actually, this rotation is of the same order of magnitude of the rotation due to the deformation of the front suspension.

In Table 4, a comparison between the linear model of Eq. (39) and the multi-body model for the 4 × 4 driveline is shown. The comparison between the total pitch given by the analytical model and total pitch given by the multi-body model provides satisfactory results. Actually the aim of the analytical model is that of explaining the physical phenomenon and not providing accurate numerical results.

The comparison gives a maximum error of 0.1 deg. But the actual error given by neglecting tyre compliance is even smaller. Actually the results given in bold characters in Table 4 give an error of 0.05 deg produced by the analytical model. So the total pitch error (0.14–0.04 = 0.1 deg) is affected by 0.05 deg only due to having neglected tyre

Table 4
Pitch due to tyre deformations. 4 × 4 driveline, comparison between the linear model of Eq. (39) and the multi-body model. Data in Table 1, k_{tf} = 250,000 N/m, k_{tr} = 300,000 N/m.

	Accel. [g]	h_{sf} [mm]	Anti-dive percentage (%)	Analytical linear model			Multi-body model	
				Pitch – susp. dive [°]	Pitch – Eq. (39) [°]	Pitch – total [°]	Pitch – Rigid tyres [°]	Pitch – Def. tyres [°]
Brakes on the hubs, horiz. arms	−0.3	450	>100	−0.15	0.36	0.21	−0.16	0.18
	−0.5	450	>100	−0.46	0.60	0.14	−0.51	0.04
Brakes on the hubs, 100% anti-dive	−0.3	350.0	<100	0.09	0.36	0.45	0.11	0.45
	−0.5	350.0	100	0.00	0.60	0.60	0.00	0.57

deformation. Finally, we can state that in the considered cases, Eq. (39) gives an error of the pitch angle due to tyre deformations within 0.05° with respect to the computation given by the multi-body model.

7. Conclusion

In this paper, the anti-dive and anti-lift conditions for a farm tractor with suspended front axle have been extensively analysed. Both the steady- and transient-state deceleration of the farm tractor has been computed by taking into account the driveline, considering the cases of 4×2 and 4×4 drivelines. The tractor and a tractor-implements combination have been considered.

Referring to anti-dive, all the possible configurations of the brake system have been considered. The 4×2 farm tractor anti-dive behaviour is very similar to that of a car. When a 4×4 driveline is considered, the behaviour of the farm tractor is very complex. In fact, the anti-dive condition is function of the longitudinal forces acting at the front and rear axles. Since the driveline is non statically determined, the longitudinal forces vary during the manoeuvre and the setup of the anti-dive configuration of the suspension is very difficult. The work presented in the paper provides different possibilities for further work. A straightforward extension is the inclusion of a trailer and/or deformable implements that can affect the system dynamic behaviour.

Appendix 1. Suspension longitudinal kinematics – 2D study

Suspension kinematics involves the three-dimensional study of the motion of the wheel with respect to the car body. Energetic or vectorial approaches can be followed for the derivation of the equations describing such motions [4,5,8]. A simplified approach, which nevertheless can give an informative and accurate representation of the behaviour of the suspension, is the analysis of the suspension kinematics by projecting the suspension links to one plane (longitudinal, transversal and horizontal) at a time [4,16]. In this way, simple 2D models can be employed and the main suspension characteristics can be promptly understood. Two-dimensional models can be used to define the poles of the suspension. The transversal (also called front view) and the longitudinal (also called side view) planes contains the most useful information [17]. In particular, by considering the longitudinal plane the pitch pole of the suspension can be computed and anti-dive and anti-lift information can be derived [17]. The longitudinal plane is defined by the longitudinal and vertical axes passing through the centre of the wheel.

Considering the suspension kinematic, the wheel hub is connected to the body by means of control arms. Each control arm is connected to the body and to the wheel hub by means of spherical joints (either actual spherical joints or rubber bushings). Each of the lines connecting a spherical join on the wheel hub to a corresponding spherical joint, belonging to the same arm, on the body represents a kinematic link. The projection of such lines on the considered plane, represent the locus of the centre of rotation of the hub with respect to the body. The lines representing the links usually intersect in a point which represent a pole of the linkage [17]. By connecting the pole with the hub, the linkage modelling in the longitudinal plane considered in the paper can be obtained. Figs. A1.1–A1.3 show this representation for three different suspension schemes actually employed on farm tractors.

Appendix 2. Multibody model of the farm tractor and validation

In this appendix, the farm tractor model, based on a proprietary computer code, used for the numerical validation of the analytical formulae presented in the paper is described. The model is divided into sub-modules, each module represents a vehicle sub-system (Fig. A2.1), which interacts with the other ones by means of input–output variables. The model is fully described in [13,15].

The model is constructed by assembling the following modules.

- Body/chassis module. The vehicle body/chassis dynamic behaviour (six degrees of freedom) is modelled.

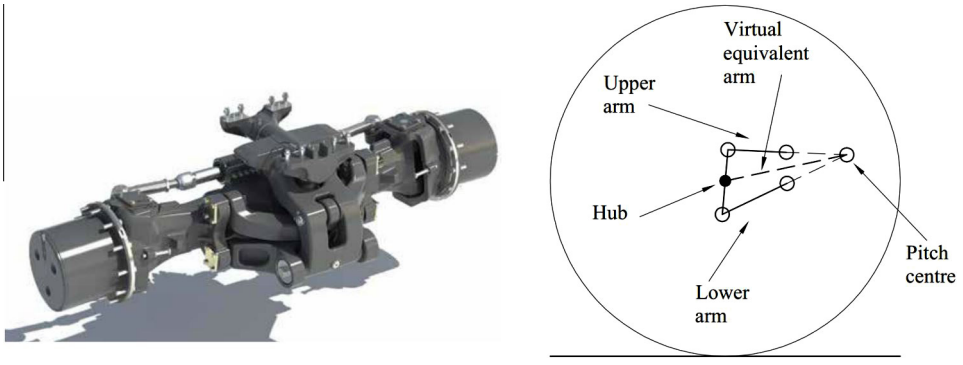

Fig. A1.1. Rigid axle longitudinal double wishbone suspension. Left: front axle of a Massey Ferguson MF8700 tractor (adapted from [18]). Right: kinematic scheme in the longitudinal plane.

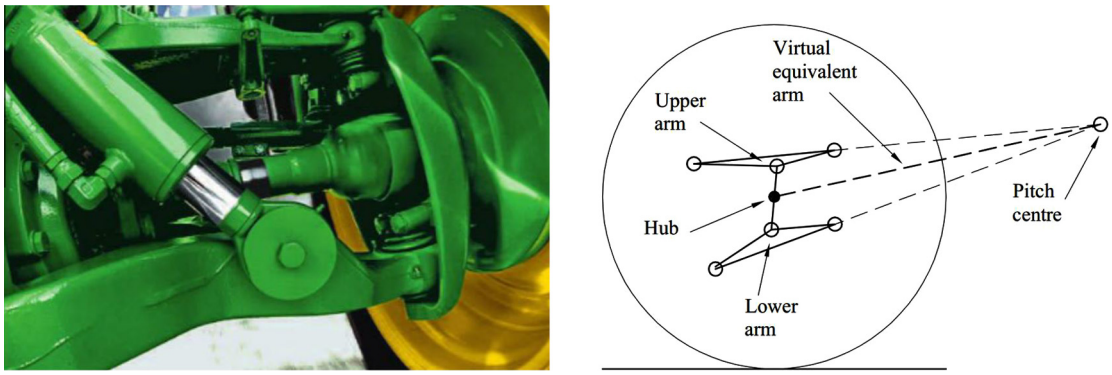

Fig. A1.2. Independent double wishbone suspension. Left: implementation on a John Deere series 8r tractor (adapted from [19]). Right: kinematic scheme in the longitudinal plane.

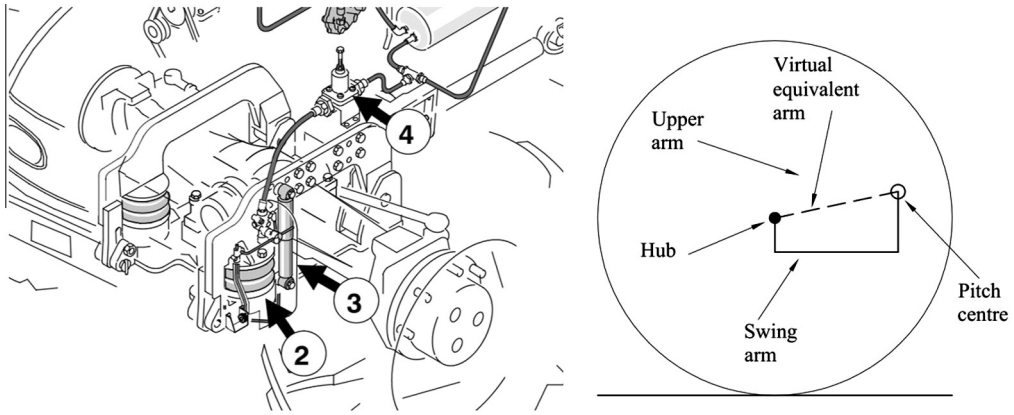

Fig. A1.3. Rigid axle swing arm suspension. Left: implementation on a Valtra T Advanced tractor (adapted from [20]). Right: kinematic scheme in the longitudinal plane.

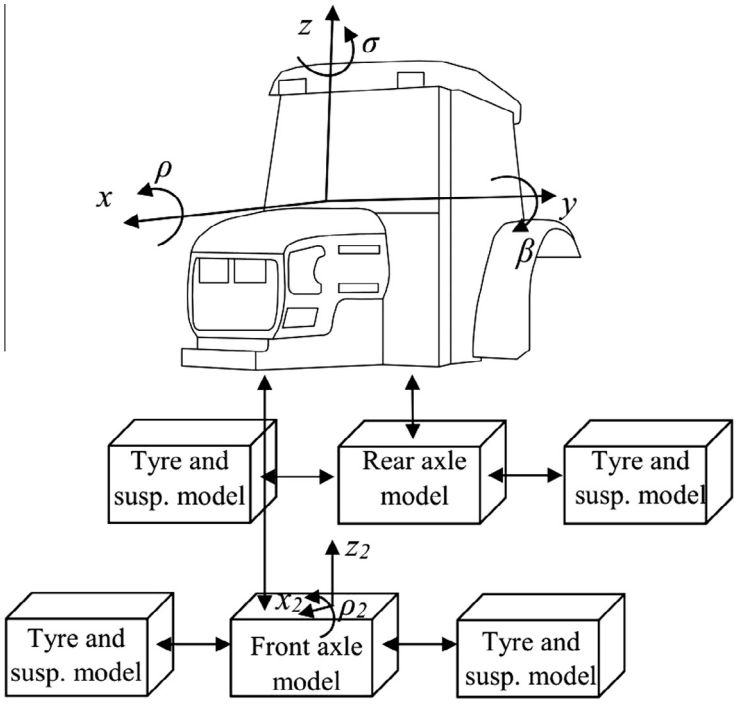

Fig. A2.1. Vehicle model (the arrows refer to input–output variables of each sub-module).

- Front axle module. The relative displacements between the front axle and the body/chassis are described. Mass and inertia tensor of the front axle are considered. It can be a live axle, but independent suspensions can also be implemented.
- Rear axle module. The relative displacements between the rear wheels and the body/chassis are described. Conventional farm tractors have no rear suspension, and so this module is available for future developments.
- Tyre modules. Four modules define the characteristic of the farm tractor tyres.
- Engine module. The engine characteristic is defined by means of the output torque as a function of engine speed and throttle position.
- Driveline module. The driveline system is outlined. In this module, the elastic and dynamic features of the driveline are taken into account.
- Steering system module. The steering mechanism is introduced. The considered farm tractor has a Jeantaud steering linkage with hydraulic actuation.
- Brake module. It defines the brake torque acting on each wheel.

The contact forces are computed by means of a single point contact model based on Pacejka's '89 Magic Formulae [21]. The transient behaviour of the tyres is taken into account both in lateral and in longitudinal direction. The behaviour of the tyres when working with combined slip is considered combining the pure longitudinal and pure cornering characteristics. An obstacle enveloping model, based on the one presented in [22,23], is used to reproduce the tyre behaviour for long and medium wavelengths (up to 30 Hz). The considered tyre model have proved to give a good simulation of the behaviour of the vehicle in on road condition and on pre-compacted soft terrain.

The tyre model has been tuned by measuring the contact force both on-road and off-road. An instrumented wheel hub has been constructed at the technical university of Milan (Politecnico di Milano) to measure accurately the force/moments on a rotating tyre [14] on the basis of the six-axis load cell presented in [24–26]. The wheel hub allows to record the six components of the contact force at the tyre/ground interface.

To ensure a good dynamic response of the models, by using the so called InTenso test-rig built at the Department of Mechanical Engineering of the technical university of Milan (Politecnico di Milano) [27], the inertia properties of the reference vehicle have been measured, within a prescribed tolerance. The maximum error on the measured main diagonal components of the inertia tensor is less than 2%.

Different manoeuvres have been considered in order to validate the two tractor models on road, off road and while passing over an obstacle [15]. The reference farm tractor (Same Dorado F75) has been instrumented by means of accelerometers and gyros in order to record the accelerations and angular velocities of the vehicle, a fifth wheel has been employed to record its absolute velocity, an instrumented wheel hub has been used to measure the forces acting on the tyres and a z-folded load cell has been fitted on the towing cable when hauling a trailer. For validation purposes, the steer signal together with the vehicle speed recorded by the fifth wheel (at the beginning of the manoeuvres) are used as inputs to the model, the other recorded signals are compared with the outputs of the model. In Fig. A2.2 the lateral and longitudinal forces during a change of lane manoeuvre while hauling a braking trailer on pre-compacted soil are shown. From this figure, it can be seen how the model is able to correctly simulate the contact force even in such a harsh environment, proving the reliable modelling of the driveline properties of the vehicle. Further validation, including other off-road, on road and passing over obstacles manoeuvres, can be found in [15].

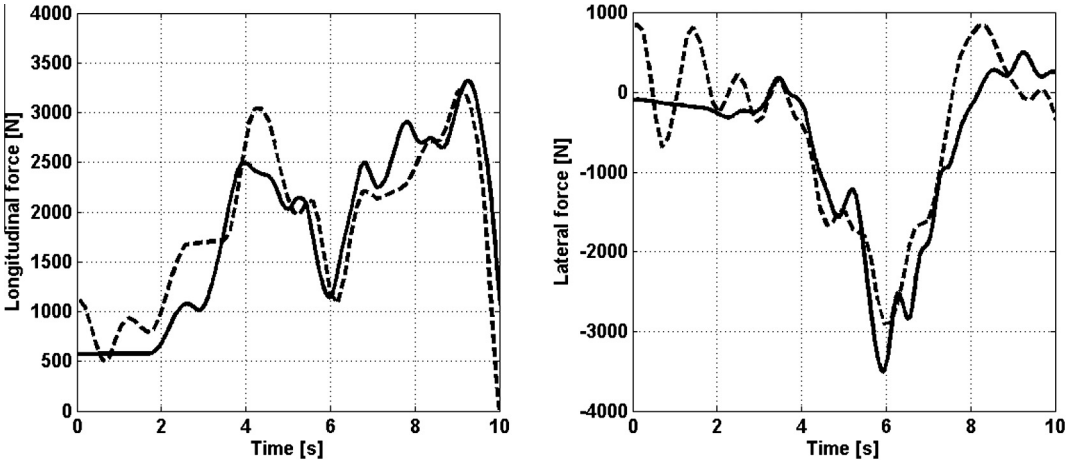

Fig. A2.2. Lane change while hauling a trailer, soft terrain, speed 1.2 m/s: longitudinal (left) and lateral (right) forces on the instrumented wheel; computed data (solid line) and measured data (dashed line).

References

[1] Mitschke M. Dynamik der Kraftfahrzeuge. Berlin: Springer Verlag; 2004.

[2] Sharp RS. Influences of suspension kinematics on pitching dynamics longitudinal maneuvering. Veh Syst Dyn 2000;33(Suppl.):23–36.

[3] Azman M, Rahnejat H, King PD, Gordon TJ. Influence of anti-dive and anti-squat geometry in combined vehicle bounce and pitch dynamics. Proc Inst Mech Eng Part K J Multi-body Dyn 2004;218(4):231–42.

[4] Morelli A. Progetto dell'autoveicolo (Car vehicle design, in Italian). Turin: Celid; 1999.

[5] Matschinsky W. Road vehicle suspensions. London: Professional Engineering Publishing; 2000.

[6] Heißing B, Ersoy M. Chassis handbook: fundamentals, driving dynamics, components, mechatronics, perspectives. Berlin: Springer; 2011.

[7] Dixon JC. Tires, suspension and handling. 2nd ed. Troy: SAE International; 1996.

[8] Matschinsky W. Suspension systems. In: Mastinu G, Ploechl M, editors. Road and off-road vehicle system dynamics handbook. Boca Raton: CRC Press; 2014. p. 727–68.

[9] Cantoni CMD, Cesarini R, Mastinu G, Previati G, Sicigliano R. Brake systems dynamics. In: Mastinu G, Ploechl M, editors. Road and off-road vehicle system dynamics handbook. Boca Raton: CRC Press; 2014. p. 837–918.

[10] Wong JY. Terramechanics and off-road vehicle engineering. Terrain behaviour, off-road vehicle performance and design. 2nd ed. Oxford: Butterworth-Heinemann; 2010.

[11] Grott M, Biral F, Sorniotti A, Oboe R, Vincenti E. Simulation for the development of an active suspension system for an agricultural tractor. SAE Int J Commer Veh 2010;2(2):12–26.

[12] Previati G, Gobbi M, Mastinu G. Multi-objective-reliability-based optimisation of a farm tractor front axle suspension. Int J Heavy Veh Syst 2011;18(3):257–71.

[13] Mastinu G, Gobbi M, Previati G, Ribaldone M. Advances in farm tractor modeling and simulation. In: IMECE international conference. Washington, US; 2003.

[14] Gobbi M, Aiolfi M, Pennati M, Previati G, Levi F, Ribaldone M, et al. Measuring forces and moments acting at farm tractor pneumatic tyre. Veh Syst Dyn 2005;43(1):412–3.

[15] Previati G, Gobbi M, Mastinu G. Farm tractor models for research and development purposes. Veh Syst Dyn 2007;45(1):37–60.

[16] Genta G, Morello L. The automotive chassis. In: Components design. Mechanical engineering series, vol. 1. Berlin: Springer; 2009.

[17] Milliken WF, Milliken DL. Race car vehicle dynamics. Troy: SAE International; 1995.

[18] <http://int.masseyferguson.com/mf8700.aspx#skipbrochure>; 2014.

[19] <http://www.deere.it/it_IT/products/equipment/tractors/8r_series/8r_series.page>; 2014.

[20] <http://www.valtra.ru/extras/75.asp>; 2014.

[21] Pacejka HB, Bakker E. The magic formula tyre model. In: Proc. of the 1st tyre colloquium; 1991.

[22] Zagelaar PWA. The dynamic response of tyres to brake torque variations and road unevenesses [Ph.D. thesis]. Delft, The Netherlands: Delft University of Technology; 1998.

[23] Pacejka HB. Tyre and vehicle dynamics. Butterworth Heinemann; 2002.

[24] Mastinu G, Gobbi M, Previati G. A new six-axis load cell. Part I: Design. Exp Mech 2011;51:373–88.

[25] Gobbi M, Previati G, Guarneri P, Mastinu G. A new six-axis load cell. Part II: error analysis, construction and experimental assessment of performances. Exp Mech 2011;51:389–99.

[26] Ballo F, Gobbi M, Mastinu G, Previati G. Advances in force and moments measurements by an innovative six-axis load cell. Exp Mech 2013. http://dx.doi.org/10.1007/s11340-013-9824-4.

[27] Gobbi M, Mastinu G, Previati G. A method for measuring the inertia properties of rigid bodies. Mech Syst Sign Proc 2011;25:305–18. http://dx.doi.org/10.1016/j.ymssp.2010.09.004.